

## Integrated plasmonic lens photodetector

James A. Shackelford,<sup>1</sup> Richard Grote,<sup>1</sup> Marc Currie,<sup>2</sup> Jonathan E. Spanier,<sup>3</sup> and Bahram Nabet<sup>1,a)</sup>

<sup>1</sup>Department of Electrical and Computer Engineering, Drexel University, Philadelphia, Pennsylvania 19104, USA

<sup>2</sup>Optical Sciences Division, Naval Research Laboratory, Washington, DC 20375, USA

<sup>3</sup>Department of Materials Science and Engineering, Drexel University, Philadelphia, Pennsylvania 19104, USA

(Received 24 November 2008; accepted 31 January 2009; published online 23 February 2009)

We present a fabricated metal-semiconductor-metal (MSM) photodetector exhibiting an enhanced photocurrent by integrating a nanoscale metallic grating into its contacts. This serves to increase the incident photon flux about the aperture of the device by guiding incident photons as surface plasmon polaritons. High speed time response data shows that the device responsivity may be increased without sacrificing speed. We demonstrate both a photocurrent enhancement and responsivity increase of about 90% at the design wavelength in comparison to otherwise identical MSM photodetectors without integrated nanoscale gratings. The device retains the MSM advantages of simplicity, planarity, and monolithic integrability. © 2009 American Institute of Physics.

[DOI: 10.1063/1.3086898]

The properties of electromagnetic radiation incident upon a flat metal/dielectric interface have been the focus of extensive research effort since the pioneering work of Ritchie in 1957.<sup>1-3</sup> Utilization of modern fabrication techniques such as focused ion beam milling and electron beam lithography have led to the introduction of nanoscale structures built upon or embedded into otherwise flat metal/dielectric interfaces.<sup>4-6</sup> The inclusion of such nanostructures and physical geometries allows for the guiding as well as the localization of light through modification of the dispersion relation of the resonant collective electron oscillations sustained at the metal/dielectric interface. The collective electron oscillations or surface plasmon polaritons (SPPs) are a manifestation of incident photons coupling to free electrons in the metal at the interface. Specifically pertaining to optimizing photodetectors (PDs), finite difference time domain (FDTD) simulations have shown that the implementation of corrugations symmetrically about an aperture significantly increases the absorption cross section of the detector, which is defined as the total power absorbed by the detector material in the aperture normalized by the incident plane wave flux.<sup>7,8</sup> Furthermore, the same simulations have shown that the absorption cross section continues to increase as the number of corrugations are increased until saturation occurs with 20 corrugations on either side of the aperture for circular geometries<sup>7,8</sup> and ten corrugations for linear geometries.<sup>8</sup>

A practical application of SPP/photon interaction is provided in the integration of a plasmonic coupler consisting of concentric circular corrugations with a Si PD,<sup>9</sup> where the circularly corrugated anode concentrates 840 nm incident light about a circular aperture 300 nm in diameter. This vertical avalanche PD shows over an order of magnitude photocurrent enhancement, depending on bias, due to its plasmonic lens. Several different implementations of SPP enhanced PDs have since been demonstrated, ranging from the fabrication of a C-shaped Ge PD (Ref. 10) to the modifica-

tion of MSM PD finger interdigitation to support SPP modes.<sup>11</sup>

Here we report on a metal-semiconductor-metal (MSM) PD where the metallic cathode and anode are each modified by the deposition of a series of ten parallel linear corrugations that have been designed to selectively couple to 830 nm light and concentrate it about a narrow slit aperture of approximately 1  $\mu\text{m}$ . This device remains planar, simple to fabricate, and integrable with other optoelectronic circuitry. Time response data comparing devices with and without plasmonic lenses show the same speed but about a factor of 2 increase in photocurrent. Simulation results predict order of magnitude enhancement of sensitivity to be possible with the optimization of corrugations and slits.

Figure 1 shows an scanning electron microscopy (SEM) tilt image taken at approximately 45° with respect to normal of the MSM-PD whose contacts are each modified by the deposition of ten linear corrugations. The nanocorrugations are necessary in order to provide the momentum  $\Delta k$  required to satisfy the dispersion relation in such a way so as to allow for the collective resonant coupling between incident pho-

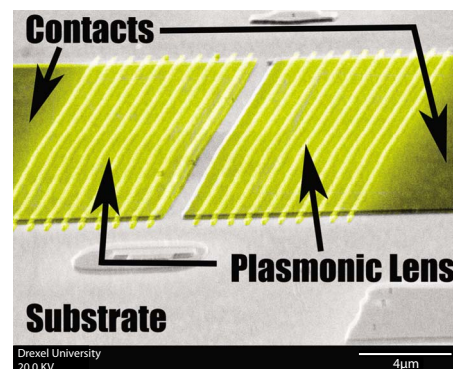


FIG. 1. (Color online) SEM micrograph of the planar integrated plasmonic lens MSM PD taken with a stage tilt of approximately 45° in respect to the device normal. The incident laser beam is directed at the device with normal incidence ( $\theta=0$ ) and is centered about the device aperture.

<sup>a)</sup>Electronic mail: bnabet@coe.drexel.edu.

tons and the electrons in the MSM-PD electrodes,<sup>2</sup> i.e.,

$$k_{\parallel} = \frac{\omega}{c} \sin \theta \pm \Delta k = \frac{\omega}{c} \sqrt{\frac{\epsilon_d \epsilon_m}{\epsilon_d + \epsilon_m}} = k_{sp}, \quad (1)$$

where

$$\Delta k = \frac{2\pi l}{a}, \quad l = 1, 2, 3, \dots \quad (2)$$

Here  $k_{\parallel}$  is the component of the incident light wave vector parallel to the device surface, the speed of light is  $c$  and its angle of incidence is  $\theta$  with respect to the device normal,  $k_{sp}$  is the surface plasmon wave vector, and  $\epsilon_d$  and  $\epsilon_m$  are, respectively, dielectric functions of air and metal—gold, in this case. Hence, grating period  $a$  is required to couple surface plasmons to normally incident light ( $\theta=0$ ) of frequency  $\omega$ . Designing for the GaAs fundamental edge of absorption around 830 nm results in a period of  $a=814$  nm for the Au/air interface. The groove to pitch ratio of the corrugations was chosen to be 1/2 and their height as  $25 \pm 5$  nm so as to increase the coupling strength of the plasmonic lens.<sup>12</sup> Remaining symbols carry the standard physical definitions. Designing for  $a$  such that coupling occurs for incident radiation of frequency  $\omega$  at angle  $\theta$  (with respect to the normal) results in photons that would normally be reflected off of the surface metal to be effectively guided to the active area of the device in the form of a surface plasmon.<sup>13,14</sup> This increases the electron hole pair generation rate which, in turn, results in an overall increase in responsivity.

The MSM PD simply consists of the as-grown undoped GaAs substrate with an absorption area of  $1 \times 30 \mu\text{m}^2$  that is also the aperture of the plasmonic lens. The device is fabricated by deposition of a 10 nm Cr adhesion layer followed by 90 nm thick Au Schottky pads forming cathode and anode. The plasmonic lens is formed by electron beam lithography on PMMA and lift-off of the 25 nm thick Au corrugations.

A large number of devices with various corrugation patterns were fabricated and tested. Time response data for typical devices comparing those with and without corrugations were taken using a Ti:sapphire laser with a pulse width of 100 fs and repetition rate of 75 MHz tuned to a wavelength of 830 nm. The laser spot was positioned at the center of the active area of the device and the resulting current transient was measured with a 40 GHz probe of a 50 GHz oscilloscope placed directly on the device contacts. The measurements were taken at room temperature with an applied bias of 5 V dc.

Figure 2 compares the time response for both a plasmonically enhanced MSM PD as well as an MSM PD without an integrated plasmonic lens. Both devices were fabricated on the same sample/substrate and are otherwise identical. The y-axis is in arbitrary units proportional to photocurrent and is identical for both panels. Results show approximately a factor of 2 increase in peak response with the addition of the plasmonic lens. The full width half maximum (FWHM) of the transient response for both devices is measured to be around 15 ps. Furthermore, the fall time for both devices is also approximately equal, which indicates that the integration of the plasmonic lens provides an increased responsivity without negatively affecting device speed.

To obtain the dependence of the photocurrent on wavelength, the same  $\approx 10 \mu\text{m}$  laser spot was placed at the center

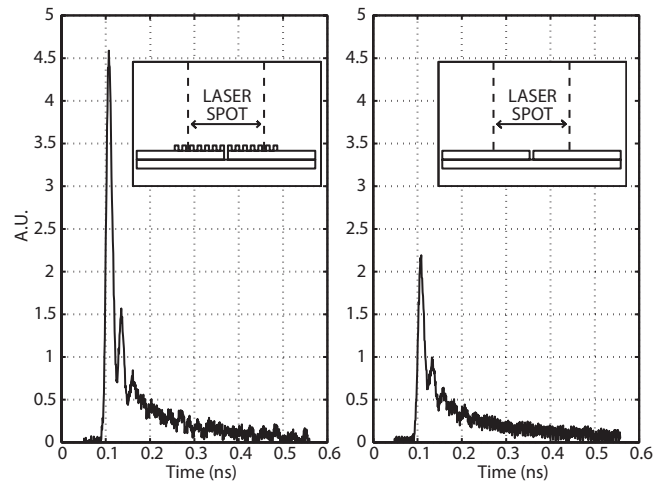


FIG. 2. Photocurrent time response to 100 fs 830 nm laser pulse of device with integrated plasmonic lens (left panel) and device without plasmonic lens (right panel). The ordinate axis scale is identical for both devices showing increased peak response for the device with integrated lens. Both devices display identical FWHM and fall time.

of the active area of the plasmonic device and the time averaged photocurrent was measured for  $\lambda=800$  nm through 870 nm at 10 nm steps. Biasing voltage of 5 V dc was placed across the device and the experiment was repeated for the MSM PD devices without corrugations. The left panel of Fig. 3 compares the experimentally obtained response of lensed and regular devices. The plasmonically enhanced PD displays wavelength selectivity, which manifests as a peak in photocurrent of  $\approx 11.8 \mu\text{A}$  at the design wavelength. By contrast, the MSM PD without plasmonic corrugations exhibits a photocurrent of  $\approx 6.1 \mu\text{A}$  for  $\lambda=830$  nm. Normalizing to the incident power, this results in device responsivities of 0.14 and 0.075 A/W, respectively. Overall, this indicates almost a factor of 2 increase in responsivity with the addition of the plasmonic lens. Incidentally, the dark current of both devices is in tens of picoamperes showing the high signal to noise ratio of these devices.

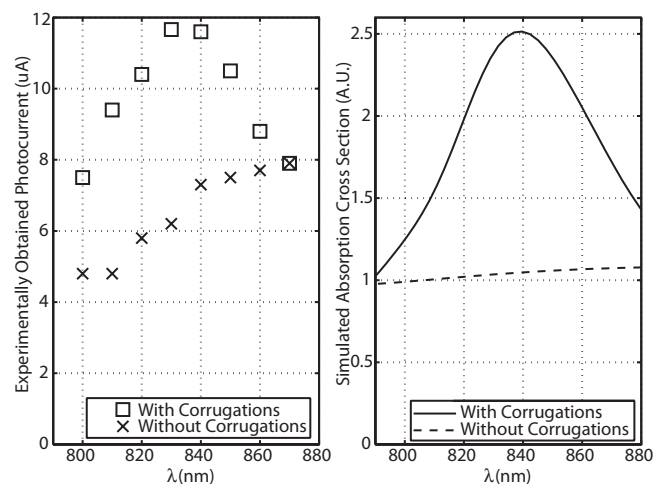


FIG. 3. (Left) Photocurrent vs wavelength for a  $10 \mu\text{m}$  laser spot centered over the active region of both PD devices. The Ti:sapphire laser was tuned in 10 nm increments and was pulsed at 75 MHz with a pulse width of 100 fs. The reported photocurrents are time averaged. (Right) Absorption cross section vs wavelength as simulated using MEEP for both MSMs with and without corrugations.

The right panel of Fig. 3 shows the simulated flux density that is guided through the aperture of lensed and regular devices using the MIT Electromagnetic Equation Propagation (MEEP) simulator, which is an open source FDTD simulation tool. This is performed by solving Maxwell's equations in two dimensions and exploiting device symmetry. Electron behavior within the metal is implemented utilizing the Drude–Lorentz model thus forming a physically accurate description of the dielectric function for Au. Simulation results closely mirror experimental data shown in Fig. 3 proving the wavelength selective guiding nature of the apertured lens.

In summary, we have designed and fabricated an integrated plasmonic PD by patterning corrugations on top of a traditional MSM PD via electron beam lithography. By exposing both the plasmonically enhanced and normal MSM PDs to a 100 fs pulsed laser, we demonstrate that the integration of the plasmonic lens does not adversely affect the speed of the response of the PD, while it considerably improves device responsivity. Furthermore, by tuning the pulsed laser through a range of wavelengths, we observe up to 90% increase in photocurrent and device responsivity at the design wavelength. Simulation results show that proper design of aperture width, corrugation pitch, duty cycle, and height can result in significant increase of responsivity. In fact, maximum enhancement, by a factor of 10.7 at 855 nm incident light, in photon flux through the aperture is predicted by proper optimization of these parameters.<sup>15</sup> Hence, addition of metallic corrugation to the contacts of an MSM PD substantially improves sensitivity of these detectors by coupling photons to surface plasmons, without any time re-

sponse penalties while maintaining all other important advantages of these devices.

For financial support, the National Science Foundation, Electronic and Photonic Devices Technology Grant No. ECCS 0702716 is acknowledged, with additional support from the Materials Sciences Division of the U.S. Army Research Office under Award Nos. W911NF-06-1-0127 and W911NF-08-1-0067.

<sup>1</sup>R. Ritchie, *Phys. Rev.* **106**, 874 (1957).

<sup>2</sup>H. Raether, *Surface Plasmons on Smooth, Rough Surfaces, and Gratings* (Springer, Berlin, 1988).

<sup>3</sup>S. Maier and H. Atwater, *J. Appl. Phys.* **98**, 011101 (2005).

<sup>4</sup>J. Weeber, Y. Lacroute, A. Dereux, E. Devaux, T. Ebbesen, C. Girard, M. González, and A. Baudrion, *Phys. Rev. B* **70**, 235406 (2004).

<sup>5</sup>W. Nomura, M. Ohtsu, and T. Yatsui, *Appl. Phys. Lett.* **86**, 181108 (2005).

<sup>6</sup>C. Chang, D. Lin, C. Yeh, C. Lee, Y. Chang, M. Lin, J. Yeh, and J. Liu, *Appl. Phys. Lett.* **90**, 061113 (2007).

<sup>7</sup>Z. Yu, G. Veronis, S. Fan, and M. L. Brongersma, *Appl. Phys. Lett.* **89**, 151116 (2006).

<sup>8</sup>R. Bhat, N. Panoiu, S. Brueck, and R. Osgood, *Opt. Express* **16**, 4588 (2008).

<sup>9</sup>T. Ishi, J. Fujikata, K. Makita, T. Baba, and K. Ohashi, *Jpn. J. Appl. Phys., Part 2* **44**, L364 (2005).

<sup>10</sup>L. Tang, D. Miller, A. Okyay, J. Matteo, Y. Yuen, K. Saraswat, and L. Hesselink, *Opt. Lett.* **31**, 1519 (2006).

<sup>11</sup>J. Hetterich, G. Bastian, N. Gippius, S. Tikhodeev, G. von Plessen, and U. Lemmer, *IEEE J. Quantum Electron.* **43**, 855 (2007).

<sup>12</sup>A. Giannattasio, I. Hooper, and W. Barnes, *Opt. Commun.* **261**, 291 (2006).

<sup>13</sup>H. Lezec, A. Degiron, E. Devaux, R. Linke, L. Martin-Moreno, F. Garcia-Vidal, and T. Ebbesen, *Science* **297**, 820 (2002).

<sup>14</sup>A. Degiron and T. Ebbesen, *Opt. Express* **12**, 3694 (2004).

<sup>15</sup>R. Grote, "Design and application of plasmonic devices," M.S. thesis, Drexel University, 2008.